

## A model for the relative humidity effect on the readings of the PM<sub>10</sub> beta-gauge monitor

C.T. Chang, C.J. Tsai\*

*Institute of Environmental Engineering, National Chiao Tung University,  
No. 75 Poai Street, Hsinchu 300, Taiwan*

Received 13 February 2003; accepted 23 June 2003

---

### Abstract

In the previous paper (Atmos. Environ. 15 (1981) 1087), we found that the PM<sub>10</sub> concentrations detected by the Wedding beta-gauge PM<sub>10</sub> monitor and those measured by the manual hi-vol PM<sub>10</sub> sampler were quite close when the ambient relative humidity (RH) was lower than the deliquescence RH (DRH) of aerosols. However, when the deliquescent point was exceeded, PM<sub>10</sub> concentrations of the beta-gauge were found to be higher and differences increased with an increasing ambient RH. In addition, theoretical water mass calculated by a thermodynamic model (ISORROPIA model, (Aquat. Geochem. 4 (1998) 123)) was found to be much higher than the actual values. In this study, models were developed to determine water evaporation loss from collected particles on the filter tape of the beta-gauge during sampling and in the monitoring room. Simulated results show that all absorbed water will evaporate completely at RH lower than about 85%. However, absorbed water does not evaporate completely at RH higher than about 85%, and remaining water in particles accounts for higher beta-gauge readings than the hi-vol concentrations. The simulated daily beta-gauge PM<sub>10</sub> concentrations are close to the actual beta-gauge readings obtained previously.

© 2003 Elsevier Ltd. All rights reserved.

*Keywords:* Beta-gauge; PM<sub>10</sub>; Aerosol mass monitor; Humidity effect

---

### 1. Introduction

There are 72 ambient air quality monitoring stations in Taiwan's air quality monitoring network, where automatic Wedding beta-gauge PM<sub>10</sub> monitors are used to measure hourly PM<sub>10</sub> concentrations. The Wedding beta-gauge PM<sub>10</sub> system has a cyclone as the PM<sub>10</sub> inlet, and the flow rate

---

\* Corresponding author. Tel.: +886-3-5731880; fax: +886-3-5727835.

E-mail address: [cjtsai@green.ev.nctu.edu.tw](mailto:cjtsai@green.ev.nctu.edu.tw) (C.J. Tsai).

**Nomenclature**

$a$	specific surface area of particle bed, $\text{m}^{-1}$
$A$	filtration area, $\text{m}^2$
$C_c$	Cunningham slip correction factor
$D$	diffusion coefficient of water vapor, $\text{m}^2 \text{s}^{-1}$
$D_p$	particle diameter, $\text{m}$
$\bar{D}_p$	average particle diameter, $\text{m}$
$DRH$	deliquescence relative humidity, %
$J_v$	evaporated flux of water vapor, $\text{kg m}^{-2} \text{s}^{-1}$
$k$	mass transfer coefficient, $\text{m s}^{-1}$
$K_2$	dust cake resistance coefficient, $\text{s}^{-1}$
$K_{2,\text{st}}$	theoretical dust cake resistance coefficient, $\text{s}^{-1}$
$L$	thickness of dust cake, $\text{m}$
$m_{\text{ev1}}$	evaporated water mass during sampling, $\text{kg}$
$m_{\text{ev2}}$	evaporated water mass during beta-counting, $\text{kg}$
$n$	ratio of cake thickness to the diameter of particle ( $L/\bar{D}_p$ )
$P_0$	pressure at upstream of sampler, $\text{N m}^{-2}$
$P_e$	Peclet number
$Q_{\text{in}}$	air flow rate at the upstream dust cake, $\text{m}^3 \text{s}^{-1}$
$Q_{\text{out}}$	air flow rate at the downstream dust cake ( $Q_{\text{in}}/(1 - \delta)$ ), $\text{m}^3 \text{s}^{-1}$
$R_{\text{R-H}}$	resistance factor, Happel's cell model
$RH$	relative humidity, %
$S_B$	saturation ratio of water vapor in monitoring room
$S_h$	Sherwood number
$S_{\text{in}}$	saturation ratio of vapor at upstream dust cake ( $\rho_{\text{in}}/\rho_e$ )
$S_{\text{out}}$	saturation ratio of vapor at downstream dust cake ( $\rho_{\text{out}}/\rho_e$ )
$u_0$	superficial fluid velocity when pressure is equal to $P_0$ , $\text{m s}^{-1}$
$V_f$	face velocity, $\text{m s}^{-1}$
$W$	mass area density of cake, $\text{kg m}^{-2}$
$x$	traveling direction of flowing fluid

*Greek letters*

$\alpha$	a dimensionless parameter in Eq. (1)
$\beta$	a dimensionless parameter in Eq. (1)
$\chi$	a dimensionless parameter in Eq. (1)
$\Delta P$	pressure drop of particle bed, $\text{N m}^{-2}$
$\Delta t$	time period of sampling, $\text{s}$
$\Delta t_B$	time period of beta-counting, $\text{s}$
$\delta$	ratio of $\Delta P/P_0$
$\varepsilon$	porosity of dust cake
$\gamma$	a dimensionless variable in Eq. (6)
$\mu$	dynamic viscosity of air, $\text{N s m}^{-2}$

$\rho$	concentrations of water vapor, $\text{kg m}^{-3}$
$\rho_e$	saturation concentration of water vapor, $\text{kg m}^{-3}$
$\rho_{\text{in}}$	concentration of water vapor at upstream of particle bed
$\rho_{\text{out}}$	concentration of water vapor at downstream of particle bed
$\rho_p$	density of particle, $\text{kg m}^{-3}$
$\sigma_g$	geometric standard deviation
$\psi$	a parameter in Eq. (7)

is 18.9 l/min. It is an equivalent method for  $\text{PM}_{10}$  designated by the US EPA. Before a sampling cycle begins, the  $^{14}\text{C}$  source of the monitor will emit beta-particles through a reference position of the filter tape. After detecting the initial or background count rate through the reference position of the filter tape, the tape is moved to the sampling position under the inlet exhaust tube and begins a sampling cycle (Wedding & Weigand, 1993). After 54 min. of the sampling cycle, the sampling manifold will start to open, and the filter tape with collected particles is returned under the  $^{14}\text{C}$  source, and the sampling manifold is closed automatically. The time that the filter tape exposes in the monitoring room as the sampling manifold opens is about 40 s. After that, the beta-gauge begins to measure the attenuated count rate for 5 min. and 20 s and the  $\text{PM}_{10}$  concentration in ambient air in that hour is estimated.

Manual Sierra–Anderson SA1200 hi-vol and Wedding hi-vol  $\text{PM}_{10}$  sampler are the designated reference methods for  $\text{PM}_{10}$  by the US EPA. Both samplers are used widely in Taiwan for ambient  $\text{PM}_{10}$  study. The Wedding hi-vol  $\text{PM}_{10}$  sampler has a cyclonic  $\text{PM}_{10}$  inlet with a flow rate of  $1.13 \text{ m}^3/\text{min}$ . Its  $\text{PM}_{10}$  inlet has been tested for particle penetration efficiency by many different tunnel facilities in the laboratory at different wind speeds (Ranade, Woods, Chen, Purdue, & Rehme, 1990). The inlet of Sierra–Anderson SA1200 is a single-stage multi-jet impactor, the flow rate is  $1.13 \text{ m}^3/\text{min}$  and has been tested in a wind tunnel (McFarland & Ortiz, 1987). Since the filter of the manual Sierra–Anderson SA1200 and Wedding  $\text{PM}_{10}$  hi-vol samples are conditioned before and after sampling, the measured concentrations are close to dry  $\text{PM}_{10}$  concentrations. According to the standard operation procedure for weighing  $\text{PM}_{10}$  filters, the average temperature of the weighting environment should be kept between  $15^\circ\text{C}$  and  $30^\circ\text{C}$ , and the temperature variation should be maintained within  $\pm 3.0^\circ\text{C}$ , whereas, the average RH of the environment should be kept between 20% and 45%, and the RH variation should be maintained within  $\pm 5.0\%$  (US EPA, 1987). Therefore, it is expected that the readings of the beta-gauge monitor will be higher than the hi-vol sampler at RH higher than DRH when aerosol particles absorbs water during sampling process of the beta-gauge monitor.

Because of the frequent occurrence of high relative humidity in the ambient air of Taiwan, the Taiwan EPA is interested to know the effect of humidity on the readings of the automatic Wedding beta-gauge  $\text{PM}_{10}$  monitors. We conducted a field study at four stations (Chung-Shan, Ta-Yuan, Chu-Shan and Ta-Liao) in Taiwan as shown in Fig. 1 and found that the  $\text{PM}_{10}$  concentrations of the Wedding beta-gauge were quite close to the measured values of manual hi-vol samplers when the ambient RH was lower than the DRH of aerosols (Chang et al., 2001). However, when the deliquescent point was exceeded,  $\text{PM}_{10}$  concentrations of the beta-gauge were found to be higher than those the manual hi-vol sampler and the differences increased with increasing ambient RH.

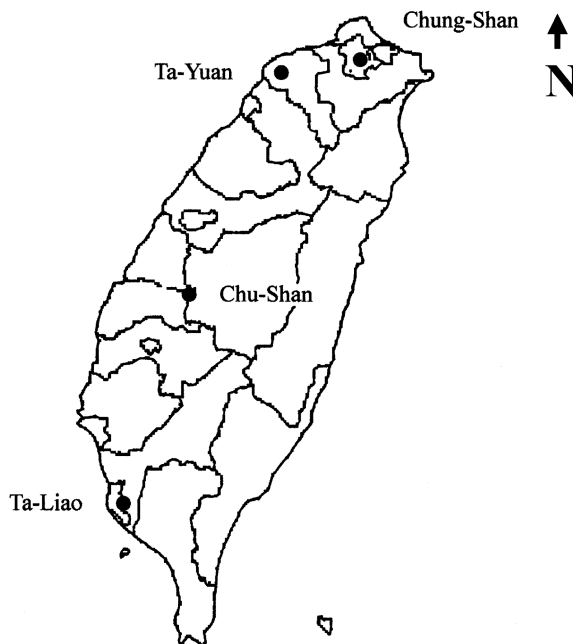


Fig. 1. The location of four sampling stations.

The experimental  $PM_{10}$  concentration ratio of beta-gauge versus hi-vol sampler in Chang et al. (2001) is further compared with the theoretical ratio assuming that the water content calculated by the thermodynamic model (ISORROPIA model, Nenes, Pandis, & Pilinis, 1998) is entirely associated in the particles of the beta-gauge monitor, as shown in Figs. 2(a) and (b). The figures show that the experimental  $PM_{10}$  concentration ratio starts to increase from 1.0 when RH is higher than 80–85%. In most cases, the thermodynamic model seems to over-predict water content in particles of the beta-gauge monitor and the difference increases with an increasing RH. Also shown in Fig. 2 is the more reasonable theoretical ratio calculated by the models that we have developed in this study. The thermodynamic model calculates the water content of particles assuming they are in thermodynamic equilibrium with a prescribed ambient condition. However, when particles are collected on a filter, water evaporation may occur due to the pressure drop through the dust cake and changes in the ambient conditions. These non-equilibrium conditions reduce the humidity effect on the beta-gauge readings.

Evaporation of volatile particulate species such as ammonium chloride and ammonium nitrate due to the evaporation when the pressure drop increases across the filter during sampling has been studied extensively (Appel & Tokiwa, 1981; Zhang & McMurry, 1987, 1992; Cheng & Tsai, 1997). However, evaporation of particle-bound water during sampling process has rarely been mentioned in the literature, despite that water can be one of the most abundant species in particles when RH is higher than DRH.

The schematic of the role of water vapor on beta-gauge readings during sampling and beta-counting is depicted in Figs. 3(a) and (b). During aerosol sampling, airborne particles absorb water when RH is greater than DRH. However, particle-bound water will evaporate during sampling mainly due to

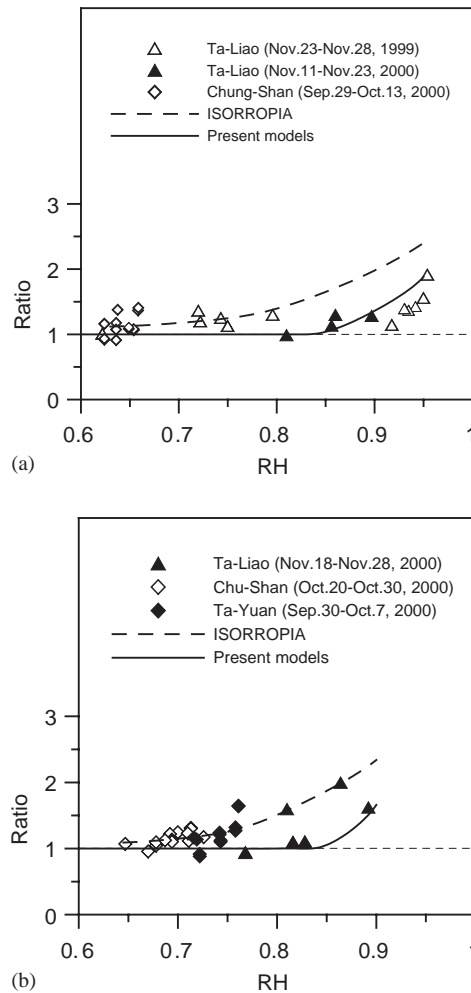


Fig. 2. Ratio of daily average PM<sub>10</sub> concentrations of Wedding beta-gauge to (a) Wedding (b) Andersen hi-vol sampler versus RH. Experimental data are in Chang et al. (2001). The long dashed line: The ratio is based on the theoretical water content of the beta-gauge calculated by the ISORROPIA model; solid line: The ratio is based on the beta-gauge concentrations calculated by the present models.

the pressure drop across the dust cake, as shown in Fig. 3(a). Before beta-counting process, the time when the sampling manifold opens for about 40 s, the dust cake is exposed to the monitoring room with air conditioning, where the humidity and temperature are most likely lower than the ambient air. Particle-bound water will evaporate during the period of 40 s. During beta-counting, the space between the filter tape and beta source or detector is very small, therefore, the amount of water evaporated will be limited, as shown in Fig. 3(b). In this study, water evaporation is assumed to be negligible during beta-counting.

In the following, models developed to calculate water evaporation of collected particles during sampling and in the monitoring room will be presented and the simulated beta-gauge concentrations will be compared with the actual readings.

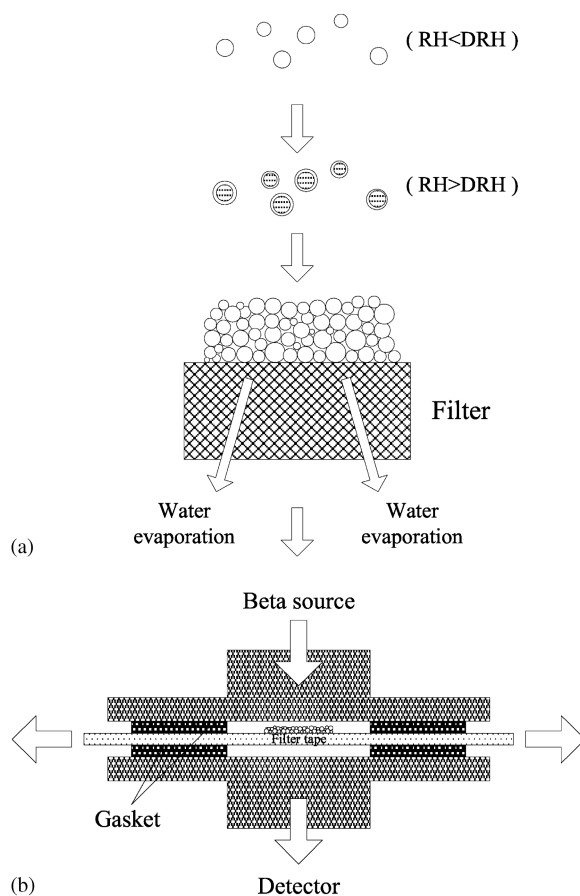


Fig. 3. (a) Water evaporation loss occurs during sampling, and (b) when the sampling manifold is opened before beta-counting. During beta-counting, evaporation loss is negligible.

## 2. Theoretical models

### 2.1. Water evaporation during sampling

To calculate the evaporated water mass in particles during sampling, the model originally developed by Cheng and Tsai (1997) is used. In the model, the evaporation loss from collected particles on the filter is considered as a mass transfer problem of a particle bed. According to the model, the saturation ratio of water vapor concentration at the downstream of the filter,  $S_{out}$ , can be calculated as

$$S_{out} = \chi + \frac{4\alpha \exp(\beta)(S_{in} - \chi)}{[(1 + \alpha)^2 \exp(\alpha\beta) - (1 - \alpha)^2 \exp(-\alpha\beta)]}, \quad (1)$$

where

$$\alpha = \sqrt{1 + \frac{4\delta}{nP_e} + \frac{24(1-\varepsilon)S_h}{P_e^2}},$$

$$\beta = \frac{nP_e}{2},$$

$$\chi = \frac{1}{1 + \frac{\delta P_e}{6n(1-\varepsilon)S_h}},$$

where  $n$  is the ratio of dust cake thickness to the average particle diameter,  $L/\bar{D}_p$ ;  $S_{in}$  the saturation ratio of water vapor at the upstream of dust cake;  $\delta$  the ratio of pressure drop across the particle bed to the pressure at the upstream of the sampler,  $\Delta P/P_0$ ; and  $\varepsilon$  the porosity of dust cake. Sherwood number,  $S_h$ , is defined as  $S_h = k\bar{D}_p/D$ ; and Peclet number,  $P_e$ , is defined as  $P_e = V_f\bar{D}_p/D$ .

The total evaporated mass of water of the collected particles during the sampling period  $\Delta t$  can be found as

$$m_{ev1} = \rho_e(S_{out}Q_{out} - S_{in}Q_{in})\Delta t, \quad (2)$$

where  $Q_{in}$  is the flow rate at the upstream of dust cake;  $Q_{out}(=Q_{in}/(1-\delta))$  the flow rate at the downstream of dust cake; and  $\rho_e$  the saturation concentration of water vapor. Other details of the model can be found in Cheng and Tsai (1997).

During sampling, water evaporation is calculated based on the pressure drop,  $\Delta P$ , through the particle cake, which can be calculated as

$$\Delta P = K_2 W V_f,$$

$$K_2 = K_{2,st} R_{R-H} = \frac{18\mu}{\rho_p \bar{D}_{P,21}^2 C_c} \cdot \frac{3 + 2(1-\varepsilon)^{5/3}}{3 - 4.5(1-\varepsilon)^{1/3} + 4.5(1-\varepsilon)^{5/3} - 3(1-\varepsilon)^2},$$

$$\bar{D}_{P,21} = \left[ \frac{\int_0^\infty D_P^3 f_0(D_P) dD_P}{\int_0^\infty D_P f_0(D_P) dD_P} \right]^{1/2}, \quad (3)$$

where  $K_2$  is the dust cake resistance coefficient,  $W$  the mass area density of cake,  $V_f$  the face velocity, and  $C_c$  the Cunningham slip correction factor. The flow resistance,  $K_2$  can be found by multiplying the theoretical dust cake resistant coefficient,  $K_{2,st}$ , by a correction factor  $R_{R-H}$  based on the Happel's cell model (Gupta, Novick, Biswas, & Monson, 1993).

## 2.2. Water evaporation in the monitoring room

To determine the evaporation loss of particle-bound water in the monitoring room during the period when the sampling manifold is opened before beta-counting, the convection–diffusion equation of the dust cake has to be solved. Neglecting the convection term, the governing equation for

the dust cake is

$$D \frac{d^2 \rho}{dx^2} + ak(\rho_e - \rho) = 0. \quad (4)$$

To solve Eq. (4), the boundary conditions for a packed bed are used

$$\rho = S_{\text{out}} \rho_e \quad \text{at } x = 0, \quad (5a)$$

$$\frac{d\rho}{dx} = 0 \quad \text{at } x = L. \quad (5b)$$

The concentration of water vapor in the dust cake can be calculated as

$$\rho(x) = \frac{(S_B - 1)\rho_e}{1 + e^{2\sqrt{\gamma}L}} (e^{\sqrt{\gamma}x} + e^{2\sqrt{\gamma}L} e^{-\sqrt{\gamma}x}) + \rho_e, \\ \gamma = \frac{ak}{D}, \quad (6)$$

where  $S_B$  is the saturation ratio of water vapor in monitoring room. Applying the Fick's law at the surface of the dust cake (at  $x = 0$ ), the evaporated flux  $J_v$  of water vapor can be found as

$$J_v = \left( \frac{e^{2n\psi} - 1}{e^{2n\psi} + 1} \right) (1 - S_B) \frac{\rho_e D \psi}{D_p}, \\ \psi = \sqrt{6(1 - \varepsilon)S_h}. \quad (7)$$

The total evaporated water mass of the collected particles during beta-counting,  $\Delta t_B$ , can be shown as

$$m_{\text{ev}2} = \left( \frac{e^{2n\psi} - 1}{e^{2n\psi} + 1} \right) (1 - S_B) \frac{\rho_e D \psi}{D_p} A \Delta t_B. \quad (8)$$

In the above models, the data of the hourly relative humidity and temperature were obtained from the Central Weather Bureau in Taiwan, and the actual readings of the automatic Wedding beta-gauge monitor of the four stations were obtained from the Taiwan EPA. The mass median of aerodynamic diameter (MMAD) and geometric standard deviation  $\sigma_g$  were measured by a micro-orifice uniform deposit impactor (MOUDI) to be 0.47 and 1.19  $\mu\text{m}$  for fine particles, and 3.10 and 1.54  $\mu\text{m}$  for coarse particles, respectively. The diffusion coefficient of water vapor is calculated according to Chapman and Enskog theory (Poling, Prausnitz, & O'Connell, 2001) and equals 0.25  $\text{cm}^2/\text{s}$  at 20°C.

A BET surface analyzer (Micromeritics ASAP 2000) was used to measure the specific surface area and porosity of the dust cake on the filter tape in the beta-gauge. The average porosity of particle cake of six samples was found to be  $0.66 \pm 0.09$ . Further, temperature and RH in the monitoring room of the automatic Wedding beta-gauge monitor was measured to be  $24.2 \pm 3.2^\circ\text{C}$  and  $69.8 \pm 10.1\%$  in this study during beta-counting.

### 3. Results and discussion

#### 3.1. Simulated results of water evaporation

The theoretical hourly dry  $\text{PM}_{10}$  concentration and ionic concentration obtained in Chang et al. (2001) were used in the thermodynamic model to calculate the theoretical water content, and



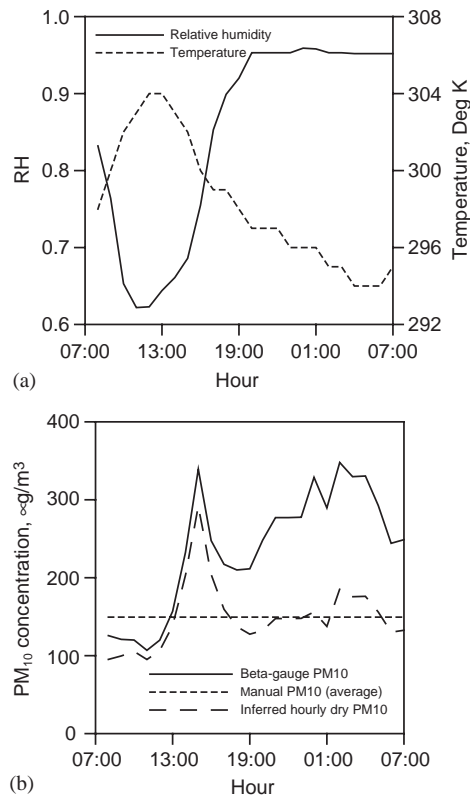


Fig. 4. (a) Temperature and relative humidity, and (b) PM<sub>10</sub> concentration versus time at Ta-Liao, November 23, 1999.

in the present models to calculate the evaporated water mass of dust cake during sampling and beta-counting. Two 1-h periods were taken as an example at Ta-Liao station in November 23, 1999 to explain the detailed variation of particle and water mass with time during the 1-h period of sampling and beta-counting. RH and temperature at Ta-Liao in November 23, 1999 are shown in Fig. 4(a). The first 1-h period is from 11:00 am–12:00 pm, when RH and temperature are about 62.3%, and 303.6 K, respectively. Water content is shown to be low in Fig. 5(a). The second 1-h period is from 2:00–3:00 am in November 24, 1999, when RH equals 95.3% and temperature is 295.2 K. Water content is as high as  $180.8 \mu\text{g m}^{-3}$  as shown in Fig. 5(b).

In Fig. 5(a) when RH is around 62.3%, water absorbed by particles, which are collected on the filter tape of the beta-gauge, evaporates entirely during sampling, and the actual reading of beta-gauge ( $120.9 \mu\text{g m}^{-3}$ ) is close to the theoretical concentration ( $106.6 \mu\text{g m}^{-3}$ ). PM<sub>10</sub> mass, water mass and evaporated water mass shown in Fig. 5 are calculated from PM<sub>10</sub> concentration, flow rate and sampling time (Fig. 4b). In comparison, if water evaporation is not considered, the sum of dry PM<sub>10</sub> concentration and water content calculated by the thermodynamic model,  $143.28 \mu\text{g m}^{-3}$ , is higher than the actual beta-gauge reading.

When RH = 95.3%, the water content is very high and if water evaporation is not considered, the theoretical beta-gauge concentration will be much higher than the actual reading, as shown

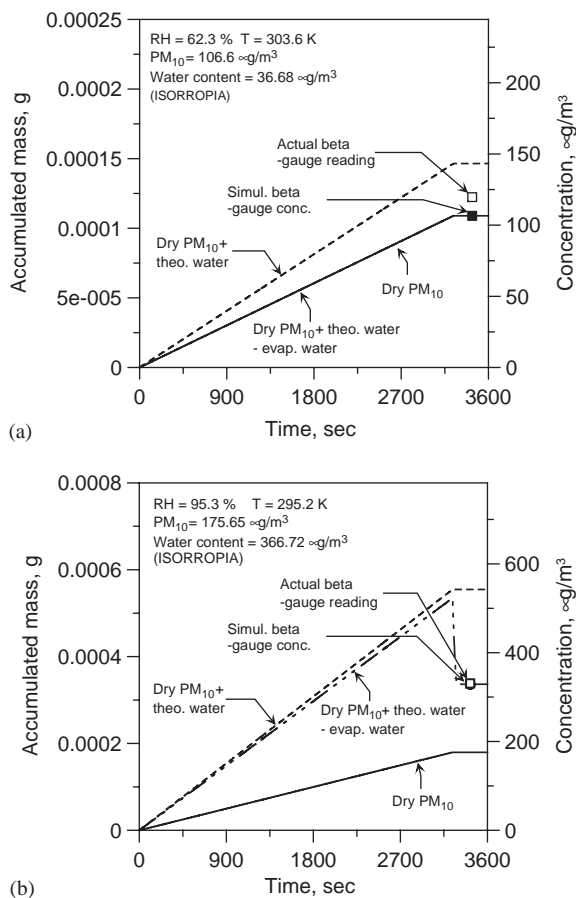


Fig. 5. Simulated PM<sub>10</sub> mass in the beta-gauge versus time during sampling and beta-counting at Ta-Liao, (a) 23rd, November 1999 (11:00 am–12:00 pm) (b) 24th, November 1999 (2:00–3:00 am).

in Fig. 5(b). Only a small fraction of water is found to evaporate during sampling. However, an appreciable amount of water in particles is evaporated during the period when the sampling manifold is opened before beta-counting. The simulated beta-gauge concentration, 336.39  $\mu\text{g m}^{-3}$  (range: 290.57–377.61  $\mu\text{g m}^{-3}$ ), is found to be very close to the actual reading, 329.7  $\mu\text{g m}^{-3}$ .

### 3.2. Comparison between simulated and actual beta-gauge concentrations

The comparison between the hourly simulated beta-gauge concentrations and the actual readings is shown in Figs. 6(a) for high ambient RH and aerosol water content area (Ta-Liao in November 23, 1999), and Fig. 6(b) for low ambient RH and aerosol water content area (Chung-Shan in October 29, 2000). Three cases assuming the average, highest and lowest RHs (70%, 80% and 60%) in the monitoring room are also calculated. Here the actual hourly beta-gauge readings are obtained from the Taiwan EPA, the simulated beta-gauge concentrations equal the sum of hourly dry PM<sub>10</sub> concentration (Chang et al., 2001) and the hourly theoretical water content calculated by the

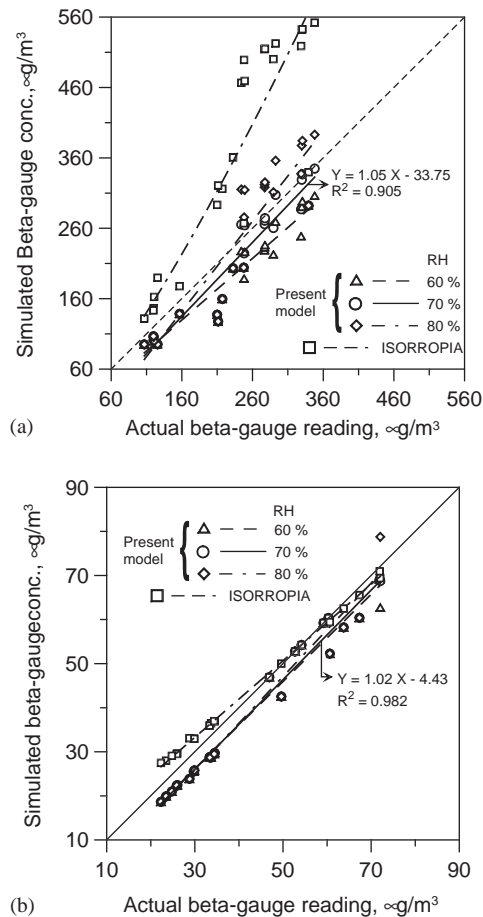


Fig. 6. Comparison between the hourly simulated and actual beta-gauge concentrations versus RH in the monitoring room, (a) Ta-Liao (November 23, 1999) (b) Chung-Shan (October 29, 2000).

thermodynamic model, minus the hourly evaporated water mass calculated by the present models. Also indicated in the figures with data points labeled “ISORROPIA” are the theoretical concentrations without considering water evaporation, and water content is calculated by the thermodynamic model.

In Fig. 6(a), the simulated beta-gauge concentrations considering water evaporation based on the present models are found to be very close to the actual readings. The slight differences between the simulated beta-gauge concentrations and actual readings are because that the theoretical hourly dry  $\text{PM}_{10}$  concentrations used in the models are predicted rather than actual values (Chang et al., 2001). In comparison, the simulated beta-gauge concentrations without considering water evaporation (“thermodynamic model”) are found to be much higher than the actual readings. Therefore, it is very important in the model to consider water evaporation loss. Part of water evaporation occurs during sampling, a good fraction occurs in the monitoring room when the sampling manifold is opened before beta-counting. RH in the monitoring room has a limited influence on the beta-gauge

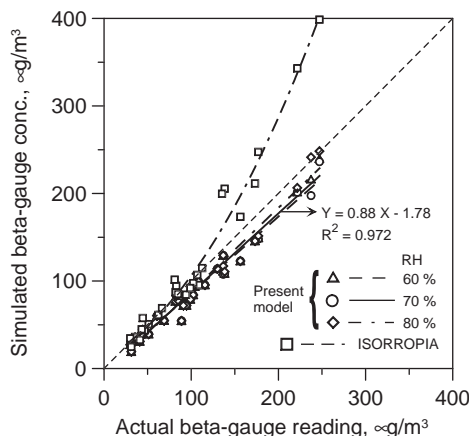


Fig. 7. Comparison between the daily simulated and actual beta-gauge concentrations versus RH in the monitoring room. Data are from all four monitoring stations.

concentrations. At the maximum RH of 80% in the monitoring room when it is closer to the ambient RH of 95.3%, the amount of water evaporation is reduced, and the simulated beta-gauge concentrations increase. In contrast, at the minimum RH of 60%, the simulated beta-gauge concentrations decrease because of the increase in water evaporation loss.

When the ambient RH is low, the amount of water content absorbed by particles is limited, whether or not water evaporation is considered in the model is not very important. As shown in Fig. 6(b) for Chung-Shan station where RH is low, the simulated beta-gauge concentrations are found to be close to the actual readings. The simulated beta-gauge concentrations without considering water evaporation loss (“thermodynamic model”) are found to be slightly higher than those considering water evaporation loss (present models). All water absorbed by particles almost evaporates completely during sampling. The influence of RHs (60%, 70% and 80%) in monitoring room on beta-gauge readings is limited.

The daily beta-gauge readings from the four monitoring stations (Chang et al., 2001) are pooled together and compared with the simulated beta-gauge concentrations, as shown in Fig. 7. The simulated beta-gauge concentrations of the present models are very close to the actual readings and the RH influence in the monitoring room is small. When the  $\text{PM}_{10}$  concentrations are lower than  $100 \mu\text{g m}^{-3}$ , the simulated beta-gauge concentrations without considering water evaporation (“thermodynamic model”) are very close to the actual readings because water content is low. However, the simulated beta-gauge concentrations are higher than the actual readings when the  $\text{PM}_{10}$  concentrations are higher than  $100 \mu\text{g m}^{-3}$  and the corresponding water content is also high.

Further simulation shows that the water absorbed by particles is evaporated entirely when RH is lower than about 85%. When RH is higher than 85%, water in particles does not evaporate entirely and remaining water will increase with increasing RH. This explains why the beta-gauge concentration is higher than the hi-vol sampler, and experimental  $\text{PM}_{10}$  concentration ratio of beta-gauge versus hi-vol sampler is increased appreciably higher than 1.0 as RH is increased from 85%, as shown in Fig. 2.

#### 4. Conclusions

In this study, models were developed to calculate water evaporation loss from particles of the beta-gauge during sampling and in the monitoring room. The simulated beta-gauge concentrations are very close to the actual readings. Although particles absorb significant amount of water when RH is higher than DRH, evaporation loss of water during sampling and in the monitoring room occurs such that actual beta-gauge readings are much lower than the theoretical PM<sub>10</sub> concentrations considering particle deliquescence alone. When the ambient RH is low, the amount of water absorbed by particles is small and is evaporated entirely during sampling. When the ambient RH is higher than DRH, particles will absorb water. Only a small fraction of water is evaporated during sampling, while an appreciable amount of water in particles is evaporated when the sampling manifold is opened before beta-counting. Remaining water in particles explain the reason why the beta-gauge readings are higher than the concentrations of hi-vol sampler when RH is higher than 85%, and the differences increase with an increasing ambient RH (Chang et al., 2001).

#### Acknowledgements

Authors would like to thank for the support of the Taiwan NSC under the contract number NSC 90-2211-E-009-027.

#### References

- Appel, B. R., & Tokiwa, Y. (1981). Atmospheric particulate nitrate sampling errors due to reactions with particulate and gaseous strong acids. *Atmospheric Environment*, *15*, 1087–1089.
- Chang, C. T., Tsai, C. J., Lee, C. T., Chang, S. Y., Cheng, M. T., & Chein, H. M. (2001). Differences in PM<sub>10</sub> concentrations measured by beta-gauge monitor and hi-vol sampler. *Atmospheric Environment*, *35*, 5741–5748.
- Cheng, Y. H., & Tsai, C. J. (1997). Evaporation loss of ammonium nitrate particles during filter sampling. *Journal of Aerosol Science*, *28*(8), 1553–1567.
- Gupta, A., Novick, V. J., Biswas, P., & Monson, P. R. (1993). Effect of humidity and particle hygroscopicity on the mass loading capacity of high efficiency particulate air (HEPA) filters. *Aerosol Science and Technology*, *19*, 94–107.
- McFarland, A. R., & Ortiz, C. A. (1987). *Aerosol sampling characteristics of the Sierra-Anderson Model 1200 PM<sub>10</sub> inlet*. Aerosol technology laboratory report No. 4716/01/08/81/ARM, Texas A& M University, College Station, TX, (pp. 15–19).
- Nenes, A., Pandis, S. N., & Pilinis, C. (1998). ISORROPIA: A new thermodynamic equilibrium model for multiphase multicomponent inorganic aerosols. *Aquatic Geochemistry*, *4*, 123–152.
- Poling, B. E., Prausnitz, J. M., & O'Connell, J. P. (2001). *The properties of gases and liquids* (pp. 11.5–11.6). New York: McGraw-Hill.
- Ranade, M. B., Woods, M. C., Chen, F. L., Purdue, L. J., & Rehme, K. A. (1990). Wind tunnel evaluation of samplers. *Aerosol Science and Technology*, *13*, 54–71.
- U.S. EPA, (1987). *Revisions to the national ambient air quality standards for particulate matter*. 40 CFR part 50, federal register, Vol. 52. 1st July (pp. 24634).
- Wedding, J. B., & Weigand, M. A. (1993). An Automatic particle sampler with beta gauging. *Journal of Air and Waste Management*, *43*, 475–479.
- Zhang, X., & McMurry, P. H. (1987). Theoretical analysis of evaporative losses from impactor and filter deposits. *Atmospheric Environment*, *21*, 1779–1789.
- Zhang, X., & McMurry, P. H. (1992). Evaporative losses of fine particulate nitrates during sampling. *Atmospheric Environment*, *26A*, 3305–3315.